



INSTITUTE of  
HYDROLOGY  
The Preprograms to the Institute of  
Hydrology Distributed Model







**Report No. 103**

**The Preprograms to the  
Institute of Hydrology  
Distributed Model**

**L. G. Watts**

**August 1988**



# Contents

	page
INTRODUCTION	
PROGRAMS MET AND GLI	2
2.1 Definition of variables	2
2.2 Model description	7
2.3 Data required	12
CASE STUDY SIMULATIONS	14
3.1 Cefn Brwyn, 25/6/80, grass	14
3.2 Tanllwyth, 1/11/77, forest	16
3.3 Tanllwyth, 7-8/2/76, two days of data	17
3.4 Cefn Brwyn, 25/6/80, using two zones	18
3.5 Gwy, 17-19/11/81, using Cefn Brwyn AWS data	19
3.6 Gwy, 8-11/2/82, using Eisteddfa Gurig AWS data	19
3.7 Tanllwyth, 7-10/2/76, using daily AWS data	20
3.8 Tanllwyth, 3 periods in 1986, comparison of EP with measured daily net rainfall	20
3.9 Tanllwyth, 11-12/1/80, using rain and snow model	23
COMMENT	24
ACKNOWLEDGEMENTS	25
REFERENCES	25



## **Abstract**

The physically-based Institute of Hydrology Distributed Model (IHDM) requires rainfall as input to generate predicted stream hydrographs. The aim of the IHDM preprograms is to estimate net (that is, effective) rainfall as an improvement over using gross rainfall as input to the main IHDM. This report describes these preprograms, together with a number of case studies of forest and grass catchments. These case studies demonstrate first that the preprograms can provide good agreement between modelled and measured net rainfall, thus generating confidence in the predictive qualities of the modelling; second, that due to restricted data availability, daily rather than hourly Automatic Weather Station data may be incorporated; third, that a complex catchment may be simulated by increasing the number of physically-based zones specified, and fourth, that a combined rain and snow model may be used.





# 1. Introduction

MET and GLI, the two programs described in this report, convert raw precipitation data into effective precipitation, that is the water input at the ground surface, by modelling the processes of interception, evapotranspiration and snowmelt. The programs were developed at the Institute of Hydrology as an aspect of physically-based rainfall-runoff modelling. In the form presented here they can be used as preprograms to the Institute of Hydrology Distributed Model which simulates both surface and subsurface catchment runoff processes.

The IHDM is a numerical, physically-based and distributed rainfall-runoff model incorporating equations of surface and subsurface flow with a physical basis, and allowing for the spatial distribution of catchment variables (Beven *et al.*, 1987). The present version of the model, IHDM4, involves the solution of the Richards equation of saturated and unsaturated components of subsurface flow by finite elements using a Galerkin weighted residuals method. Kinematic wave representations of channel flow and overflow are solved by a finite difference scheme. In such a distributed model it is advantageous to be able to provide accurate estimates of the spatial and temporal variability of effective precipitation input. MET and GLI can also be employed for the conversion of gross to net precipitation for other analytical or modelling purposes.

Program MET (Meteorological input) modifies automatic weather station (AWS) data to a form appropriate for use in a particular catchment and in sub-regions of that catchment. These sub-regions or 'zones' are chosen to represent the spatial differences which may occur over the area of interest, in particular in terms of elevation, slope aspect and angle and vegetation type. In MET, corrections are made relating to slope and altitude; those which depend on surface properties are made in GLI.

Program GLI (Ground Level Inputs) determines the flux of water at the ground surface. For rainfall, the processes of interception, evapotranspiration and throughfall are considered, but not stemflow. When used in conjunction with the IHDM, surface and root zone evaporative losses are considered in the main program. For snow conditions, melt is modelled either by an energy budget method or by a temperature index method.

Section 2 of this report defines the variables used in the pre-programs, details the structure of the FORTRAN programming and includes examples and formats of data files. Section 3 describes the results of case studies using the pre-programs.

## 2. Programs MET and GLI

### 2.1 DEFINITIONS OF VARIABLES

#### *MET*

ADEP	°C	Wet bulb depression, measured by AWS
ALT	m	Altitude of each elevation zone
ANETF	$J m^{-2} s^{-1}$	Net radiation, measured by Funk radiometer
ARAD	$J m^{-2} s^{-1}$	Solar radiation, measured by AWS
ARF	$mm h^{-1}$	Rainfall, measured by AWS
ARNET	$J m^{-2} s^{-1}$	Net radiation, measured by AWS
ATA	°C	Air temperature, measured by AWS
ATW	°C	Wet bulb temperature, measured by AWS
AZ	degrees	Angle for each radiation zone type
CATCH		Name of the catchment
CNET	$J m^{-2} s^{-1}$	Corrected net radiation
CRAD	$J m^{-2} s^{-1}$	Corrected solar radiation
CSOL	$J m^{-2} s^{-1}$	Corrected direct solar radiation
DC	°C	Dry bulb temperature correction
DEC	degrees	Declination of sun on first day of month
DECMIN	degrees	Minimum declination of the sun
DELS	$mbar °C^{-1}$	Slope of saturated vapour pressure-temperature curve
DF		Cosine of minimum angle for altitude of sun
DLAP	$°C m^{-1}$	Dry bulb temperature lapse rate
DPT	°C	Dew point temperature, measured by AWS
DR		Factor to convert degrees to radians
DSOL	$J m^{-2} s^{-1}$	Corrected diffuse solar radiation
E		Parameter for determining vapour pressure
EQT	minutes	Correction to mean solar time on first day of month
ESAT	mbar	Saturated vapour pressure over water at temperature TA
ESATW	mbar	SVP over water at temperature TW
F		Parameter for determining vapour pressure
FACT		Factor for deriving corrected solar radiation from measured solar radiation
G		Constant dependent on cloud type: 0.4 = high cloud cover 0.6 = medium cloud cover 0.9 = low cloud cover
GC	°C	Dew point temperature correction factor
GLAP	$°C m^{-1}$	Lapse rate for dew point temperature
HA	degrees	Hour angle
HAWS	m	Altitude of AWS
HOUR	radians	Hour angle
HZONE	hours	Difference between time used for AWS data and GMT
IDAY		Day of month that data starts

IDEW		0 = no dew point temperature data available 1 = dew point temperature data available
IDIFF		0 = no diffuse solar and no net radiation data 1 = net but no diffuse solar radiation data 2 = diffuse solar and net radiation data available
IEV		Array with elevation number corresponding to each zone
IFIN		Temporary storage for number of days in month
IH		Hour of the day
IMONTH		Month that data starts
INTRVL		0 = hourly AWS data available 1 = only daily AWS data available (if INTRVL = 1, NH = number of days of AWS data and IH = date of the month)
IRAD		Array with radiation type number for each zone
IRAIN		0 = use AWS rainfall data 1 = use river gauging station or areal catchment rainfall data, rather than AWS rainfall data
LONG	degrees	Longitude
NDAY		Number of days in month
NEV		Number of elevation zone types (4 or less)
NH	hours	Number of hours of AWS data
NOON	hours	Nearest integer hour to true solar noon
NRAD		Number of radiation zone types
NZONE		Number of zones (8 or less)
P		Correction factor for direct solar radiation on a slope
P0	mbar	Atmospheric pressure
QA		Specific humidity of air at height ZA
QD		Saturated specific humidity over water at temperature TA
QW		Saturated specific humidity over water at temperature TW
RAD	$J m^{-2} s^{-1}$	Measured solar radiation
RF	$mm h^{-1}$	Precipitation rate
RNET	$J m^{-2} s^{-1}$	Measured net radiation
SC	$J m^{-2} s^{-1} K^{-4}$	Stefan-Boltzman constant
SMIN	hours	Time between true solar hour and nearest integer hour
SNOON	hours	True solar noon
TA	$^{\circ}C$	Air temperature
TDEW	$^{\circ}C$	Corrected dew point temperature
THETA	degrees	Latitude
TW	$^{\circ}C$	Wet bulb temperature
VF		Vapour pressure factor
WC	$^{\circ}C$	Wet bulb correction factor
WLAP	$^{\circ}C m^{-1}$	Wet bulb temperature lapse rate
WS	$m s^{-1}$	Wind speed measured by AWS

X		Cosine of angle between direction of sun and zenith direction
X1		Sine of angle of sun at noon above horizon of flat plain at latitude THETA and declination of sun
X2		Constant in equation for diffuse solar radiation
ZEN	degrees	Zenith angle for each radiation zone type

## GLI

ALB		Shortwave albedo for snow
ALT	m	Altitude of elevation zone type
AS1, AS2, AS3		Parameters of empirical equation for snow albedo
AV		Albedo of vegetation after snowmelt
C	$J m^{-2} s^{-1}$	Sensible heat transfer at snow surface
CATCH		Name of catchment
CKEFF	$J m^{-1} K^{-1} s^{-1}$	Thermal conductivity of snow
CLAI		Leaf area index
CMAX	mm	Maximum interception storage
CNET	$J m^{-2} s^{-1}$	Corrected net radiation
CPA	$J kg^{-1} K^{-1}$	Specific heat of air
CPI	$J kg^{-1} K^{-1}$	Specific heat of ice at constant pressure
CPLAI		Product of CLAI and PLAI
CPW	$J kg^{-1} K^{-1}$	Specific heat of water at constant pressure
CRAD	$J m^{-2} s^{-1}$	Corrected solar radiation
CS	mm	Interception storage
D	$m s^{-1}$	Bulk turbulent transfer coefficient
DELS	$mbar ^\circ C^{-1}$	Slope of saturated vapour pressure-temperature curve
DN	$m s^{-1}$	Bulk turbulent transfer coefficient, corrected for stability
DRAIN	mm	Drainage from vegetation (in 1 hour period)
EE	$kg m^{-2} s^{-1}$	Evaporation at upper surface of snow
EH	$J m^{-2} s^{-1}$	Heat required to produce evaporation
EINT	$m hr^{-1}$	Evaporation rate of intercepted water
EP	$m hr^{-1}$	Rate of input of water to ground surface (that is, effective or net precipitation as input to IHDM)
EQ	$kg m^{-2} s^{-1}$	Evaporation rate from snow
ESATI	mbar	Saturated vapour pressure over ice at TSURF
FACT	m	For snow: factor for calculating snow surface temperature from heat and flux For rain: factor in Penman-Monteith calculations
G		Cloudiness parameter in Brunt equation
GF	$J m^{-2} s^{-1}$	Geothermal heat flux

H	$J m^{-2} s^{-1}$	Total energy flux to snow
HOUR	hours	Time since last snowfall
HVEG	m	Height of vegetation
H1	$J m^{-2} s^{-1}$	Energy flux from air to snow
IDAY, IMONTH, IYEAR		Start time of data
IEV		Elevation zone type number
IH		Hour of the day
INET		0 = if corrections for the type of surface are to be made to the AWS data 1 = if measured net radiation is available and the surfaces properties of all zones in the catchment are the same as those of the AWS
INTRVL		0 = hourly AWS data available 1 = only daily AWS data available (if INTRVL = 1, NH = number of days of AWS data and IH = date of the month)
IRAD		Radiation zone type number
IT		Time taken for water to flow through snowpack
IVEG		Vegetation zone type number
LVW	$J kg^{-1}$	Latent heat of vaporisation of water
LWI	$J kg^{-1}$	Latent heat of fusion of water
MODEL		1 = for energy budget snowmelt model 2 = for temperature index snowmelt model
NEV		Number of elevation zone types (4 or less)
NH		Number of hours of data
NOUT		Type of output: if NOUT = 1 full details of net radiation and energy budget components are printed
NRAD		Number of radiation zone types
NVT		Number of vegetation zone types (3 or less)
NZONE		Number of zones (20 or less)
PLAI		Proportion of ground covered by vegetation
PE	$m hr^{-1}$	Potential evaporation
PNET	$mm h^{-1}$	Throughfall
P0	mbar	Atmospheric pressure for each elevation zone type
QA		Specific humidity of air at height ZA
QD		Saturated specific humidity at dry bulb temperature
QI		Saturated specific humidity over ice at temperature TSURF
QINT	$mm h^{-1}$	Input to the canopy store
QW		Saturated specific humidity at wet bulb temperature
RA	$kg m^{-3}$	Density of air
RADJ		Adjustment factor for back radiation from snow for effect of vegetation and cloudiness (if no cloudiness data available)
RF	$mm h^{-1}$	Rate of rainfall input
RICH		Richardson number for atmospheric stability
RN	$J m^{-2} s^{-1}$	Heat supplied to snow by rainfall
RNET	$J m^{-2} s^{-1}$	Net radiation

RS	$\text{kg m}^{-3}$	Density of snow
RUTB		B parameter in Rutter model
RUTK		K parameter in Rutter model
RW	$\text{kg m}^{-3}$	Density of water
SC	$\text{kg m}^{-2}\text{s}^{-1} \text{K}^{-4}$	Stefan-Boltzmann constant
SF	$\text{mm h}^{-1}$	Rate of snowfall
SHD		Difference in specific humidities between snow surface and height ZA
SMR	$\text{m s}^{-1}$	Snow melt rate
SUMRO		Sum of output values
SW	$\text{mm h}^{-1}$	Water equivalent of snowfall rate
T	$^{\circ}\text{C}$	Initial temperature of snowpack
TA	$^{\circ}\text{C}$	Air temperature at height ZA above snow
TABS	K	Value of TA
TS	$^{\circ}\text{C}$	Average temperature of snowpack
TSURF	$^{\circ}\text{C}$	Surface temperature of snowpack
T2	$^{\circ}\text{C}$	Average temperature of snowpack at forward time step
VF		Emmissivity of atmosphere
W	$\text{m s}^{-1}$	Wind speed at height ZA above ground
WE	m	Water equivalent of snowpack
WE0	m	Initial water equivalent of snowpack
WS	$\text{m s}^{-1}$	Wind speed at height ZB above surface
ZA	m	Height of temperature measurements above the ground
ZB	m	Height of wind speed measurements above the ground
ZET	m	Aerodynamic roughness length
ZPD	m	Zero plane displacement
Z0	m	Aerodynamic roughness length for snow for model 1, temperature index for model 2



## 2.2 MODEL DESCRIPTION

### *MET*

A description of the MET program, is provided here, section by section.

1. Description of variables.  
A listing of the variable names and definitions, including units, is given.
2. Definitions of arrays.  
Arrays are dimensioned, and double precision is declared.
3. Ephemeris of the sun.  
To calculate direct solar radiation on a slope, the declination of the sun, DEC, and the correction to mean solar time, EQT, are defined in data statements for the first day of each month (abstracted from Smithsonian Meteorological Tables). NDAY, the number of days in each month, is also declared.
4. Read constants for the catchments.  
The name of the catchment CATCH, latitude THETA (positive for degrees north of equator), longitude LONG and difference between local time and Greenwich Mean Time (GMT), HZONE (both positive for degrees east of Greenwich), are read. The number of zones, NZONE, required to model the catchment, and the number of elevation types, NEV, and of radiation types, NRAD, are read. Each zone is allocated both an elevation and radiation type number, IEV and IRAD respectively, and an altitude, ALT, is defined for each elevation type. The effect of shading on direct solar radiation is calculated from definitions of the minimum declination of the sun, DECMIN, and the cosine of the minimum angle for which the sun can still illuminate the catchment, DF (from Smithsonian Meteorological Tables). For the slope of each radiation zone type, a gradient, ZEN, and an aspect, AZ (measured in an easterly direction from north), are defined.
5. Read constants for the meteorological station.  
Data for the AWS are read. INTRVL defines whether hourly or only daily AWS data are available. HAWS gives the altitude of the AWS, IDAY and IMONTH the initial day and month of the data to be used, and NH the number of data records.
6. Determine temperature correction factors.  
Lapse rates for wet bulb temperature WLAP, dry bulb temperature DLAP, and dew point temperature GLAP are read in, and correction factors for each elevation zone are calculated as the product of the lapse rate and the altitudinal difference between that zone and the AWS.
7. Calculate air pressure for each elevation type.  
The air pressure for each elevation zone type, P0, is calculated from  $P0 = 1.012 \times 10^3 (1 - 0.0065 \times ALT/288)^{5.2553}$
8. Step through calculations at hourly intervals.  
Subsequent calculations are performed for each hour of data (or day of data if only daily AWS data are available).
9. Determine the solar noon and hour angles.  
If hourly data are available, diffuse radiation varies throughout a day and is calculated by determining the time of solar noon, SNOON (depending on longitude, time of year and local time difference from

GMT), and the hour angle, HA (a measure of rotation from the solar noon position).

10. Read the AWS data.

AWS data may comprise hour of day IH, solar radiation ARAD, net radiation ARNET, wet bulb depression ADEP, air temperature ATA, wind speed WS, and rainfall ARF. There are options for reading hourly or daily data, and for using rainfall data at a river gauging station or areal catchment rainfall data in preference to AWS rainfall data.

11. Correct wet and dry bulb and dew point temperatures.

For each elevation zone type, wet bulb TW and dry bulb TA temperatures are calculated from the AWS wet bulb depression ADEP, and AWS dry bulb temperature ATA, and lapse rate correction factors.

12. Calculate specific humidity for the air.

For each elevation zone type, the saturated vapour pressure over water, ESAT, and the saturated specific humidity, QD, corresponding to air temperature TA are determined from the empirical relationship (Beven, 1979)

$$ESAT = 0.003 \times TEMP^4 + 0.063 \times TEMP^3 + 0.776 \times TEMP^2 + 5.487 \times TEMP + 17.044$$

where

$$TEMP = TA/5 - 3$$

and

$$QD = 0.62197/(P0 (1.0045 \times ESAT) - 0.37803)$$

Similarly, QW, the saturated specific humidity at temperature TW is calculated.

Then

$$QA = QW - 0.0005 (TA - TW)$$

DELS, the slope of the saturation vapour pressure-temperature curve is given by

$$DELS = (0.622 \times DESAT \times P0 / 1.0045) / (P0 / 1.0045 - 0.378 \times ESAT)^2$$

where

$$DESA = 0.0024 \times TEMP^3 + 0.0378 \times TEMP^2 + 0.3104 \times TEMP + 1.0974$$

13. Calculate vapour pressure factor for Brunt equation.

The vapour pressure factor, VF, for the Brunt equation (Brunt 1932; Sellers 1965, p.53) is calculated from

$$VF = E + F (ESAT/1.333)^{0.5}$$

where E and F are empirical constants.

14. Calculate correction for direct solar radiation.

The direct solar radiation correction factor for gradient and aspect of each radiation zone type is found by calculating the angle between the direction of the sun at a given hour and the orientation of the ground surface.

15. Correct direct and diffuse solar radiation.

Direct solar radiation is corrected using the factor calculated in the previous section. The diffuse component is corrected using ZEN and FACT, the ratio of diffuse to total solar radiation falling on a horizontal plane, where

$$FACT = DF + (1-DF)(X-X1)/(X2-X1)$$

where DF is the cosine of the minimum altitude of the sun, X is the cosine of the angle between the direction of the sun and zenith, X1 is the sine of the angle of the sun at noon above the horizon of a flat surface, and X2 is a constant.

16. Prepare data file for GLI.

Two output data files are set up, which will be used as input data for

GLI. The first file contains VF, DELS and QD for each elevation zone type. The second file contains corrected solar radiation, CRAD, corrected net radiation CNET, air temperature TA, specific humidity of air QA, windspeed WS, and rainfall RF.

## *GLI*

The corrected meteorological data calculated in MET are now used to calculate interception and evapotranspiration and/or snowmelt. The emphasis in the present report is towards interception and evapotranspiration; more detailed treatment of the snowmelt model is presented elsewhere (Morris 1983, 1985).

1. Description of variables.

A listing of variable names and definitions, including respective units, is provided.

2. Define array sizes.

Arrays are dimensioned. Double precision is declared.

3. Define physical constants.

Densities of air and water, RA and RW; specific heat at constant pressure of air, water and ice, CPA, CPW and CPI; latent heat of sublimation and fusion of water, LVW and LWI; Stefan-Boltzmann constant, SC; parameters in the Brunt equation, E and F, and geothermal heat flux, GF, are defined.

4. Read constants for the catchment.

The name of the catchment CATCH, the number of zones NZONE, elevation types NEV, vegetation types NVT, and radiation types NRAD, are read. For each zone, an elevation, vegetation and radiation type number are assigned to IEV, IVEG and IRAD respectively. NOUT defines the extent of printout required. ALT, the altitude of each elevation zone type, is defined.

5. Read constants for the meteorological data.

INTRVL defines whether hourly or only daily AWS data are available. IDAY, IMONTH, IYEAR provide the initial date of the AWS data. INET specifies whether corrections for albedo and vegetation are required. ZA and ZB give heights above ground level at which bulb temperatures and wind speed, respectively, were measured. NH defines the number of data records available.

6. Read initial snow characteristics.

Two types of snowmelt model, the energy budget and temperature index models, are available. Z0 is the aerodynamic roughness length of the snow in the energy budget model, and represents the degree-hour factor in the temperature index model. Initial values of snow density RS, water equivalent WE0, and average temperature T are read. Thermal conductivity, CKEFF, is calculated from RS.

7. Read initial vegetation characteristics.

Height of vegetation HVEG, zero plane displacement ZPD, and aerodynamic roughness length ZET, are read, and are used to calculate the turbulent transfer coefficient over vegetation. The maximum interception store CMAX, Rutter model interception parameters RUTB and RUTK, leaf area index CLAI, proportion of ground covered by vegetation PLAI and albedo of vegetation AV are read. Variation of snow albedo with time may be specified using parameters AS1, AS2, AS3. RADJ is an adjustment factor for net long wave radiation, to account for

- effects of vegetation and cloudiness.
8. Initialise snow properties and interception storage.  
Interception store CS is set to zero. Surface temperature TSURF and average temperature TS are set to initial value T. Initial snowpack depth Z is calculated from initial water equivalent of snowpack.
  9. Initialise hour since last snowfall count.  
HOUR, the number of hours since the last snowfall, is set to zero.
  10. Read air pressure for each elevation zone.  
Air pressure P0 is read from a file generated by the MET program.
  11. Initialise ground level input array.  
Ground level input EP stores effective (net) rainfall or snowmelt, to be used, for example, as input to the main part of the IHDM. Since snowmelt can be lagged over time, a two-dimensional array is specified so that snowmelt can be stored for each time step.
  12. Read corrected meteorological data.  
Corrected meteorological data, comprising IH, CRAD, CNET, TA, QA, WS and RF, are read from a file generated by MET.
  13. Read further meteorological parameters.  
VF, DELS and QD are read from a file produced by MET.
  14. Calculate snowfall for each elevation zone.  
If TA is negative, then precipitation is considered to be snowfall and RF is set to zero.
  15. For each zone choose models required.  
If the snowpack depth is less than  $10^{-6}$ m and there is no snowfall, then the snowmelt models are bypassed in preference to the rainfall (interception-evapotranspiration) model. Conversely, if there is snow, the rain model is bypassed and either the energy budget (sections 16 to 24) or temperature index (section 25) model is entered.
  16. Estimate net radiation.  
INET defines whether corrections are required for the effect of different surfaces on net radiation, RNET. If no corrections are required, RNET is set to CNET. If corrections are required, then  

$$RNET = CRAD(1-ALB) + RB \times RADJ$$
 where ALB is a function of parameters AS1, AS2, AS3, and net longwave radiation RB is estimated from the Brunt equation (Brunt 1932).  

$$RB = SC(VF(TA+273)^4 - (TSURF+273)^4) (1-G)$$
  17. Calculate turbulent transfer coefficients.  
DN, the turbulent transfer coefficient, is calculated from wind speed WS, and heights above ground ZA, ZB, and Z0.
  18. Calculate sensible heat transfer.  
Sensible heat transfer at snow surface, C, is given by  

$$C = RA \times CPA \times DN (TA-TSURF)$$
  19. Calculate latent heat transfer.  
Latent heat transfer, EH, is a function of LWV, QA, DN, QI and QA, where QI is a function of P0 and TSURF.
  20. Calculate the heat supplied by rainfall.  
RN, the heat supplied to snow by rainfall, is given by  

$$RN = RW \times CPW \times TA (RF \times 0.001/3600)$$
  21. Calculate the total energy flux from the air to the snow.  
H1, energy flux from air to snow, is given by  

$$H1 = RNET + C + RN - EH$$
  22. Calculate the new snow surface temperature.  
From the heat flow equation, surface temperature TSURF is  

$$TSURF = TS + 2 \times H1 \times FACT/CKEFF$$
 where

- FACT = (CKEFF × 3600/RS × CPI × PI)<sup>0.5</sup>
23. Calculate the snowmelt rate.  
The snowmelt rate, SMR, is calculated from the energy available for snowmelt, H, after warming of the pack to melting point, divided by the product of LWI and RS.
  24. Calculate the change in snowpack depth.  
The change in snowpack depth, X, is given by  

$$X = SMR \times 3600 + EQ \times 3600/RS$$
 where EQ is the evaporation rate for snow .
  25. Calculate melt rate and change in snowpack depth.  
For the temperature index model, X is given by  

$$X = 3600 \times Z0 \times TA$$
  26. Calculate new snowpack depth and water equivalent.  
New snowpack depth is derived by subtracting X from Z. A new water equivalent, WE, is calculated.
  27. Determine the ground level input from snowmelt.  
The time lag for water flow through the pack is determined by an empirical equation. For any time step  

$$EP = EP + (SMR \times RS - EE) \times 3600/RW + RF \times 0.001$$
 where EP is the ground level input
  28. Calculate specific humidity deficit.  
In the interception-evapotranspiration model, specific humidity deficit SHD is the difference between QD and QA.
  29. Calculate turbulent transfer coefficient.  
Turbulent transfer coefficient D is a function of WS, ZET, ZPD, ZA, ZB and HVEG.
  30. Estimate net radiation.  
Net radiation is corrected for surface characteristics using the sum of net longwave radiation, RB, from the Brunt equation, and net shortwave radiation.
  31. Calculate potential evapotranspiration.  
Potential evapotranspiration, PE, is calculated based on the Penman-Monteith equation (Monteith 1965) with zero canopy resistance, using  

$$PE = (PNET \times DELS + RA \times CPA \times D (Q-QA))/(LVW(DELs + CPA/LVW))$$
  32. Calculate throughfall.  
Throughfall PNET is given by the proportion of RF which does not fall on vegetation, thus  

$$PNET = RF \times (1 - PLAI)$$
 Since the model performs calculations with an hourly time-step, if only daily RF data are available then they are averaged over a 24-hour period and hence a constant RF is input hourly to subsequent sections of the model.
  33. Calculate evaporation from a fully wetted canopy.  
When the water stored on the canopy, CS, exceeds the maximum, CMAX, canopy evaporation, EINT, is a proportion CLAI × PLAI of PE. The difference between the intercepted RF and the loss by evaporation is the input to the interception store, QINT.
  34. Calculate drainage from a fully wet canopy with positive input.  
If CS exceeds CMAX, evaporation occurs at the potential rate. The change in canopy storage with time is calculated from the Rutter interception model (Rutter *et al.* 1971). Given the time step interval, an analytical solution for the new storage, C2, after the elapsed time can

be given by

$$C2 = CMAX + (\ln-INT + CALC - \ln(QINT + CALC1 + RUTK \exp(CALC)) / RUTB$$

where

$$CALC = RUTB (CS - CMAX + QINT)$$

and

$$CALC1 = RUTK \exp(RUTB(CS - CMAX))$$

Drainage from the canopy, DRAIN, is then

$$DRAIN = CS - C2 + QINT$$

Stemflow is not explicitly incorporated (see section 3.8)

35. Calculate drainage from a fully wet canopy with negative input.

If CS exceeds CMAX, then

$$C2 = CMAX \ln(RUTB \times RUTK + \exp(-RUTB(CS - CMAX)))/RUTB$$

and

$$DRAIN = CS - C2$$

36. Calculate drainage from an incompletely wetted canopy.

If C1 exceeds CMAX, then

$$C1 = CS + RF \times PLAI - EINT$$

and

$$C2 = CMAX - \ln(RUTB \times RUTK + \exp(-RUTB(C1 - CMAX)))/RUTB$$

and

$$DRAIN = C1 - C2$$

37. Determine the net precipitation as ground level input.

$$EP = PNET + DRAIN - PE$$

38. Prepare ground level input file (for IHDM).

Write EP to a file, to be used, for example, as input data to the main IHDM.

39. Move to next time step.

## 2.3 DATA REQUIRED

This section provides some typical values for data required as input to the programs, together with a brief explanatory note.

### ***MET***

Two input data files are required. The first input file comprises AWS data (see section 2.2, MET subsection 10). An example of the second input file (here presented with parameter names) may be:

THETA = 52.5    LONG = 3.8    HZONE = 0.0  
NZONE = 1    NEV = 1    NRAD = 1  
IEV = 1  
IRAD = 1  
ALT = 442.0  
DF = 0.47    DECMIN = 23.0  
ZEN = 5.81  
AZ = 127.3  
INTRVL = 0



HAWS = 510.0 IDAY=8 IMONTH=2 NH=72 IDIFF=1 IDEW=0 G=0.6  
WLAP = 0.0065 GLAP = 0.005

This data file indicates that the catchment is at 52.5°N, 3.8°W with nil time difference with respect to GMT. The catchment is modelled using 1 zone, with 1 elevation type and 1 radiation type zone (hence IEV and IRAD are trivial, with only 1 type zone). Mean altitude of the catchment is 442 m. DF is derived from Smithsonian Meteorological Tables, and DECMIN is the minimum declination during the period of study (here from 8-10 February). Gradient is 5.81° and aspect is 127.3° from north. Hourly AWS data are available. Altitude of the AWS is 510 m; AWS data are available from 8 February; there are 72 hours of records; net but not diffuse radiation data are available; dew point temperatures are unavailable, and medium cloud cover is specified. Lapse rates are defined.

Parameters E = 0.56 and F = 0.05 are specified in a data statement.

## *GLI*

Two data files output from MET are used as input to GLI. The third input data file (together with parameter names) may be of the form:

NZONE = 1 NEV = 1 NVT = 1 NRAD = 1  
IEV = 1  
IVEG = 1  
IRAD = 1  
NOUT = 1  
ALT = 442.0  
INTRVL = 0  
IDAY = 8 MONTH = 2 NYEAR = 82  
INET = 1 ZA = 1.5 ZB = 2.0 NH = 72  
MODEL = 1  
Z0 =  $5.0 \times 10^{-3}$  RS =  $5.5 \times 10^2$  T = 0.0 AR = 0.0  
WE0 = 0.0  
HVEG = 0.1 ZPD = 0.0 ZET = 0.01 CMAX = 1.0  
RUTB = 2.0 RUTK = 0.0342 CLAI = 1.0 PLAI = 0.9  
AV = 0.2 AS1 = 0.0 AS2 = 0.0 AS3 = 0.0  
RADJ = 0.0

This data file indicates that the catchment is modelled using 1 zone, with 1 elevation type, 1 vegetation type, and 1 radiation type (hence IEV, IVEG and IRAD are trivial). Full details of radiation calculations are to be printed. The mean altitude of the catchment is 442 m. Hourly AWS data are available, from 8 February 1982. Measured net radiation is available, temperatures are measured at 1.5 m above ground and winds at 2.0 m above ground, and there are 72 records of data. The energy budget snow model is to be used in preference to the temperature index model. Aerodynamic roughness length for snow is 0.005 m, density of snow is  $550 \text{ kg m}^{-3}$ , and initial temperature is zero. Zero water equivalent for snowpack is specified. Vegetation is 0.1 m high, zero plane displacement is at the origin, aerodynamic roughness is 0.01 m of the order of one-tenth of HVEG, (Thom and Oliver 1977, Beven 1979), and maximum interception store is 1 mm. The value of Rutter B is 2.0 mm and Rutter K is  $0.0342 \text{ mm h}^{-1}$  (based on values for trees given by Calder 1977 and Rutter and Morton 1977). Leaf area index (the ratio of the

total area of potential vegetation interception surfaces to total area of ground covered by vegetation) is 1.0, and 90% of ground is covered by vegetation. An albedo of 0.2 is specified, and parameters AS1, AS2, AS3 are set to zero. The adjustment factor for radiation is set to zero.

Parameters specified within the GLI preprogram are RA=1.2, RW=1000.0, CPA=1005.0, CPW=4187.0, CPI=2093.4, LVW= $2.5 \times 10^6$ , LWI= $3.34 \times 10^5$ , SC= $5.7 \times 10^{-8}$ , E = 0.56, F = 0.05, G = 0.6, and GF = 2.0.

### 3. Case Study Simulations

A number of case studies are presented here, intended to simulate: (1) a grassland catchment, (2) a forested catchment, (3) the use of an increased number of hourly data records, (4) the use of the two zones rather than just one, (5) the incorporation of rainfall data from a river gauging station in conjunction with AWS data, (6) and (7) the use of daily rather than hourly data, (8) a comparison of modelled EP with measured net daily rainfall, and (9) the use of a combined rain and snow model.

The case studies are for storms on the Institute of Hydrology experimental catchments at Plynlimon, mid-Wales. The Severn catchment (8.7 km<sup>2</sup>) is predominantly forest, the Wye catchment (10.6 km<sup>2</sup>) is predominantly grassland. AWSs are at Cefn Brwyn and Eisteddfa Gurig (Wye) and at Tanllwyth and Carreg Wen (Severn). The catchments studied here are the Cefn Brwyn and Gwy (Wye) and Tanllwyth (Severn).

#### 3.1 CEFN BRWYN, 25/6/80, GRASS

For this small grassland catchment, parameters were initially taken as PLAI=0.9, CLAI=1.0, CMAX=1.0 mm, HVEG=0.5 m, WE0 = 0.0 m, RUTB = 2.0 mm and RUTK = 0.0342 mm h<sup>-1</sup>. All temperatures in the AWS data at Cefn Brwyn were greater than zero.

Figure 1 shows that a realistic plot of net rainfall, EP, against time was simulated. Time t=0 corresponds to midnight. From t=0-9 h, rainfall was zero which resulted in zero values and subsequently in small negative values of EP, due to potential evapotranspiration (see section 3.8). A maximum observed rainfall, RF, of 4 mm and simulated EP of 2.1 mm occur around t=11 h. EP exceeds RF at t=12-14 h due to the release of intercepted rainfall from storage. Between t=16-24 h, rainfall was zero and EP decreased from 0.3 mm to zero, simulating the tailing-off of the lagged release of intercepted RF.

Sensitivity tests were performed on the initial model parameters and the results were compared to the initial run. An inconceivably high interception store of 10.0 mm for grassland was tested, and indeed generated low EP values that

were very unlikely. Decreasing CMAX to 0.01 mm resulted in EP being unacceptably high, given the timing and characteristics of this particular storm, as a consequence of the greatly decreased storage capacity. Using HVEG = 0.1 m generated increased EP against time. CLAI = 0.1 produced a moderate increase in EP. PLAI = 0.5 produced an increase in EP, since less RF would have been intercepted. Reducing DECMIN by 10% gave rise to less than 1% change in CRAD and CNET, and little change in EP.

A simulated comparison of grassland and forest was attempted by assuming that afforestation had occurred. Parameters CMAX = 2.0 mm, HVEG = 3.0 m, ZET = 0.3 m, AV = 0.1, CLAI = 2.0, PLAI=0.75, and RUTB = 1.76 mm, RUTK = 0.0162 mm hr<sup>-1</sup> (Calder, 1977) were thought to be reasonable (see Rutter and Morton, 1977). This assumed that the forest was represented by a 75% ground cover of 3 metre high trees with 2 mm interception capacity, and the equivalent of two layers of canopy.

Figure 1 shows the modelled pattern of EP. For a total RF ( $\Sigma RF$ ) of 6.5 mm, the total EP in the forest model ( $\Sigma EP_F$ ) was 1.7 mm (26% of  $\Sigma RF$ ) and the total EP in the grass model ( $\Sigma EP_G$ ) was 4.0 mm (62% of  $\Sigma RF$ ). This clearly illustrates the different runoff responses simulated between forest and grass.  $EP_G$  always exceeded  $EP_F$ . At t=14 h both  $EP_G$  and  $EP_F$  exceed RF, due to the lag in release of intercepted rainfall. For t=6-9 h and t=19-24 h, EP is zero or negative for both grass and forest studies. The loss from the forest is greater than from grass since evapotranspiration is higher, especially in this June simulation. The differences in the response of EP to input RF are primarily the result of simulating a doubled interception store and doubled leaf area index in the afforested study.

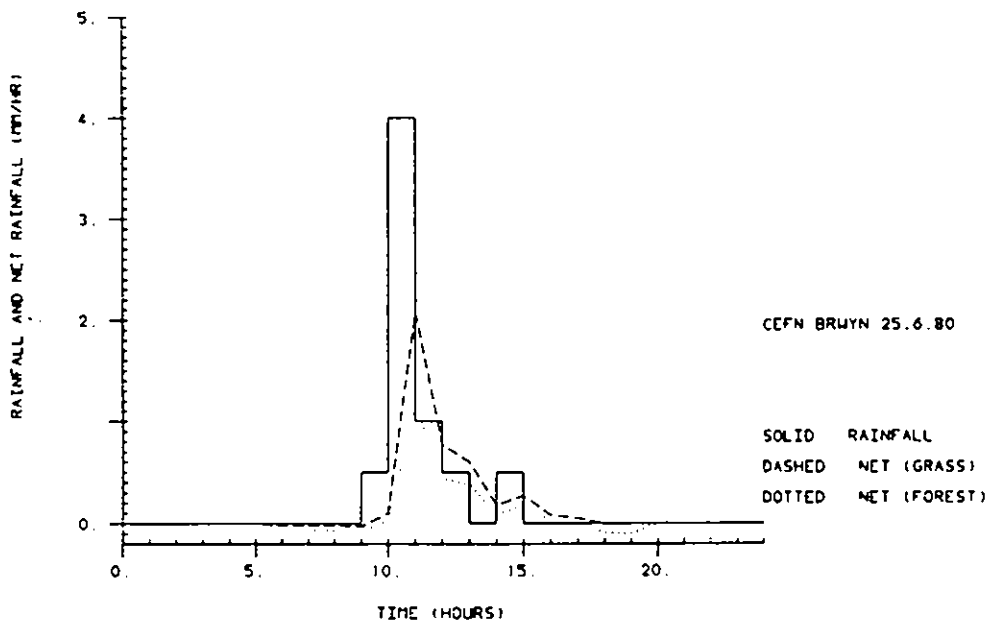


Figure 1 Rainfall and modelled net rainfall (for grass and forest) against time for the storm of 25/6/80 on the Cefn Brwyn catchment.

### 3.2 TANLLWYTH, 1/11/77, FOREST

Using parameters thought to be representative of a forested catchment (see section 3.1), the storm of 1/11/77 for the Tanllwyth (0.9 km<sup>2</sup>) was simulated.  $\Sigma RF$  was 45.5 mm in 24 hours: hence this storm was seven times more intense than that studied in section 3.1. The model generated  $\Sigma EP = 39.3$  mm (86% of  $\Sigma RF$ ). In a sensitivity test, increasing HVEG to 10.0 m produced little change, EP decreasing by only around 0.01 mm h<sup>-1</sup>.

A simulation was performed where deforestation and planting of grassland was assumed. Grassland parameters of HVEG = 0.1 m, ZET = 0.01 m, CMAX = 1.0 mm, RUTB = 2.0 mm, RUTK = 0.0342 mm h<sup>-1</sup>, CLAI = 1.0 mm and PLAI = 0.90 were defined. This simulated  $\Sigma EP = 41.8$  mm (92% of  $\Sigma RF$ ). Hence, compared with section 3.1, a much greater intensity storm gave rise to a significantly increased proportion of EP.

A further simulation, of bare soil, using parameters HVEG = 0.0, ZET = 0.001 mm, CMAX = 1.0 mm (to allow for some surface ponding), RUTB = 5.0 mm, RUTK = 0.0005 mm h<sup>-1</sup>, CLAI = 0.0 and PLAI = 0.0 was attempted, and the  $\Sigma EP$  produced was almost 100% of  $\Sigma RF$ .

Figure 2 compares the grass with the forested simulation. The peak at t=5-7 hours is similar to that generated in section 3.1. For t=1-16 h, EP<sub>G</sub> exceeds EP<sub>F</sub>. At t=7-11 h, EP is due to delayed release of interception storage. At t=12 h storage is not yet exceeded, though EP<sub>F</sub> approaches EP<sub>G</sub>. The

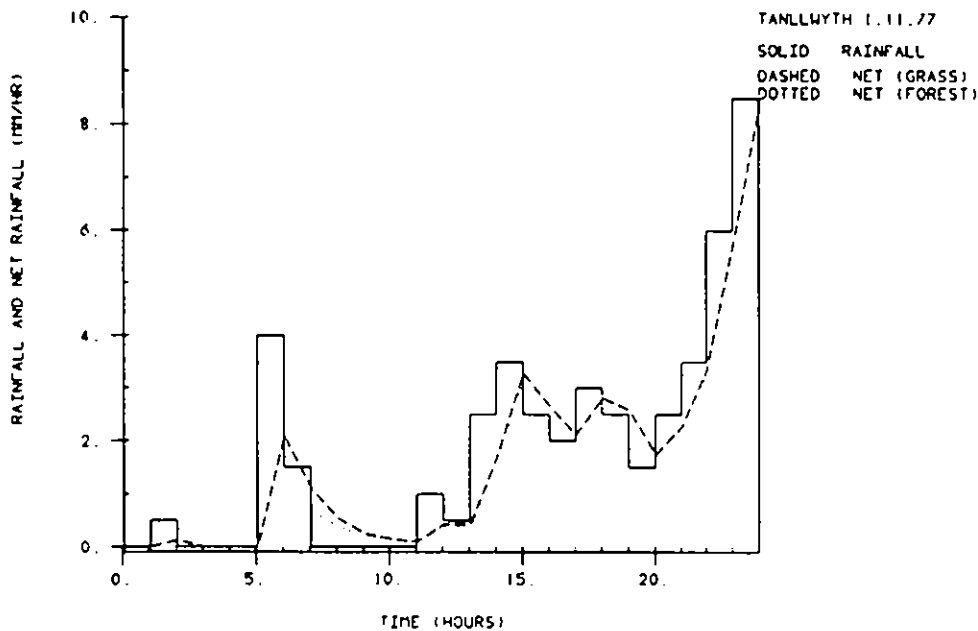


Figure 2 Rainfall and modelled net rainfall (for grass and forest) against time for the storm of 1/11/77 on the Tanllwyth catchment.

difference between  $EP_F$  and  $EP_G$  at  $t=12$  h compared with at  $t=6$  h suggests that the storage capacity of the forest is almost filled by the earlier peak at  $t=6$  h. For  $t=16-24$  h,  $EP_F$  is very similar to  $EP_G$ . Little rainfall is lost to interception-evapotranspiration, indicating that the storage capacity has been exceeded.

### 3.3 TANLLWYTH, 7-8/2/76, TWO DAYS OF DATA

This simulation used two days of hourly AWS data.  $\Sigma RF$  was 20.5 mm. A forest simulation generated  $\Sigma EP = 16.9$  mm (82% of  $\Sigma RF$ ).  $EP$  always exceeded zero and minimal evaporation was simulated. Since input surface temperatures were only 1-2 C, this suggests that little evaporation would be expected.  $\Sigma EP$  as a percentage of  $\Sigma RF$  is lower than in section 3.2, perhaps because this storm is less than one-quarter as intense as the previous storm, resulting in interception storage capacity being less readily exceeded.

A deforested simulation produced  $\Sigma EP = 18.9$  mm (92% of  $\Sigma RF$ ). Figure 3 shows that the peak occurs 1.5 hours earlier and is of 10% greater magnitude in the grass compared to the forest simulation, as a consequence of the greater interception capacity of the forest. At  $t=12-13$  h,  $EP_G$  exceeds  $EP_F$ , whereas at  $t=14-21$  h,  $EP_F$  exceeds  $EP_G$  because of the lagged response in the release of intercepted rainfall.

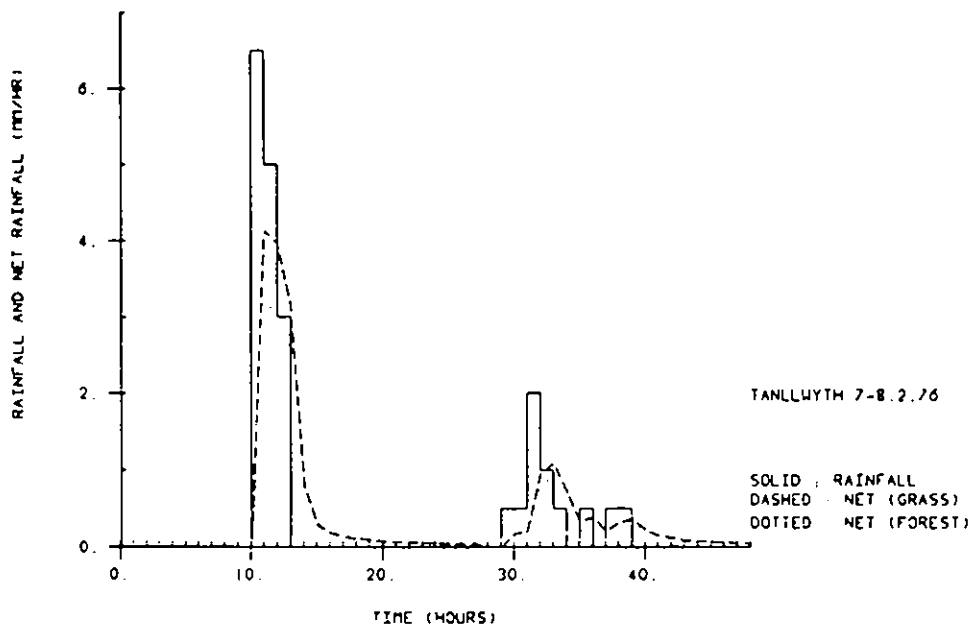


Figure 3 Rainfall and modelled net rainfall (for grass and forest) against time for the storm of 7-8/2/76 on the Tanllwyth catchment.

Table 1 compares the simulations of sections 3.1, 3.2 and 3.3 against five-year means for 1970-1975 for the Wye and Severn catchments overall. The values underlined represent the value simulated (or measured) for the existing catchment vegetation. Considering the different time scales between the simulations (namely a summer storm for the Cefn Brwyn and two winter storms for the Tanllwyth) and measurements, acceptable agreement is derived (see section 3.8).

**Table 1**  $\Sigma EP$  as a percentage of  $\Sigma RF$

Section	Catchment name and storm date	Total rainfall input mm	Bare		
			Forest	Grass	Soil
Simulations	3.1 Cefn Brwyn 25/6/80	6.5	26%	<u>62%</u>	-
	3.2 Tanllwyth 1/11/77	45.5	<u>86%</u>	<u>92%</u>	100%
	3.3 Tanllwyth 7-8/2/76	20.5	<u>82%</u>	92%	-
Anon, 1976	Wye 1970-75		n/a	<u>82%</u>	n/a
	Severn 1970-75		<u>70%</u>	n/a	n/a

### 3.4 CEFN BRWYN, 25/6/80, USING TWO ZONES

Simulation of the storm of section 3.1 was repeated, but now representing the catchment as two zones or sub-regions rather than one. The adjusted parameters used were: NZONE=2, NEV=2, NRAD=2, IEV(1)=1, IEV(2)=2, IRAD(1)=1, IRAD(2)=2, ALT(1)=413.0, ALT(2)=360.0, ZEN(1)=10.94, ZEN(2)=1.45, AZ(1)=242.0, and AZ(2)=195.0.

In the basic two-zone simulation only one vegetation zone was specified (the existing grassland), and hence NVT=1, IVEG(1)=IVEG(2)=1 were set. The simulated EP was little different from the one-zone scheme, suggesting that the one-zone scheme may be an adequate representation of the study catchment. This also indicated an apparently greater sensitivity to parameters such as vegetation rather than to the number of elevation and radiation zones in this case study. Comparing the two schemes, the value of EP at any time step using the one-zone scheme was generally intermediate between the two values generated in the two-zone scheme, thus demonstrating the averaged nature of the one-zone scheme.

Further test simulations were performed. In the basic simulation a peak EP of 2.1 mm was derived, corresponding to 52% of the peak RF. Increasing DF by 10% had no significant effect on the EP values. However, increasing RF by a factor of ten throughout the study period produced an EP peak of 37.9 mm, corresponding to 95% of peak RF. In this simulation the storage capacity has clearly been exceeded in comparison to the basic simulation. Simulating the upland zone as afforested and the lowland zone as grass led to a large difference in EP between the two zones. At peak, EP<sub>F</sub> was 29% of RF and EP<sub>G</sub> was 52% of RF. This clearly showed the effect on EP of the



larger interception capacity of forests. A further simulation assumed that both zones were afforested and generated a significant difference in EP compared with the basic simulation, with a peak  $EP_F$  29% of RF.

This case study indicates that more than one zone may be used to represent a study catchment and that different types of vegetation, elevation and radiation zones may be incorporated. Such provisions may be critical for representations of physically more complex catchments.

### 3.5 GWY, 17-19/11/81, USING CEFN BRWYN AWS DATA

In a simulation of the storm of 17-19/11/81 on the Gwy (3.9 km<sup>2</sup>), the nearest available AWS data were from Cefn Brwyn (approximately 2.8 km distant from the Gwy, with a difference in elevation of 450 m). These Cefn Brwyn AWS data were used in conjunction with rainfall for the Gwy. For  $\sum RF = 80.5$  mm, 78.1 mm of  $\sum EP$  (97% of  $\sum RF$ ) was simulated. This high percentage of rainfall being simulated as net rainfall seems reasonable for grassland since the storm is intense, and measured air temperatures are low, and hence interception storage is rapidly exceeded and there is little interception-evapotranspiration.

A simulated increase in PLAI from 0.75 to 0.90 produced a minimal change in EP, since (i) when RF was low a 20% increase in PLAI still gave less than 0.1 mm change in EP, and (ii) when RF was high EP already comprised almost 100% of RF. This result suggests that storm characteristics are critical to the simulations.

### 3.6 GWY, 8-10/2/82, USING EISTEDDFA GURIG AWS DATA

For the period studied, the nearest available AWS data for the Gwy was at Eisteddfa Gurig (approximately 1.5 km from the Gwy, with a difference in elevation of 100 m). Hourly data were available over the 72 hour period considered. Grassland parameters of HVEG = 0.1 m, CMAX = 1.0 mm, RUTB = 2.0 mm, RUTK = 0.0342 mm h<sup>-1</sup>, AV = 0.2, CLAI = 1.0 and PLAI = 0.9 were set. Since temperatures exceeded 0°C, the rain only model was used, setting WE0 = 0.0.

Figure 4 shows the measured RF and modelled EP.  $\sum RF$  was 32.5 mm,  $\sum EP$  was 27.0 mm (83% of  $\sum RF$ ). For the first 15 hours, RF was zero. This resulted in negative EP being simulated for t=9-16 h, due to potential evapotranspiration. For t=16-28 h, EP approached RF with time as maximum interception storage was approached. After the main peak, all RF was simulated as EP, indicating that the storage capacity was attained and that the shape distribution of the storm is important with regard to the timing of peak EP with respect to peak RF. Subsequently, EP exceeded RF, due to delayed runoff from the release of intercepted stored rainfall. After t=60 h the pattern was repeated, but on a smaller scale.

Comparing this storm to that described in section 3.5, both over 72 hour periods, it is clear that the more intense storm generated increased runoff because interception capacity was exceeded at an earlier stage.

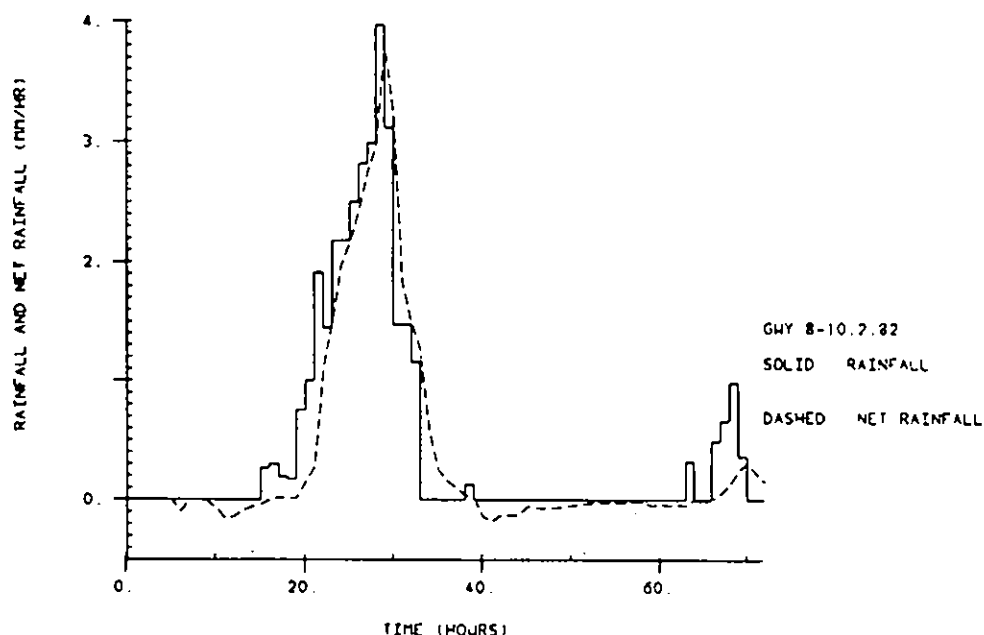


**Figure 4** Rainfall and modelled net rainfall against time for the storm of 8-10/2/82 on the Gwy catchment.

### 3.7 TANLLWYTH, 7-10/2/76, USING DAILY AWS DATA

Frequently only daily AWS data and daily measured net rainfall (necessary for comparisons with modelled EP) are available (see section 3.8). Simulations have therefore been performed using daily AWS data, requiring INTRVL = 1 to be specified. This specification results in the daily RF being divided by 24 to derive a constant mean hourly rainfall, used as input rainfall for all 24 hourly time steps. An updated interception store CS is calculated at each time step, and hence the output EP varies with each hourly time step. Daily EP is then determined by summation over the hourly EP values.

Four days of data have been analysed (NH = 4).  $\sum RF$  was 40.5 mm, and generated  $\sum EP$  of 35.5 mm (87% of  $\sum RF$ ). This value is in close agreement with the values of 86% and 82% simulated for the other winter storms of 1/11/77 (section 3.2) and 7-8/2/76 (section 3.3) respectively.

### 3.8 TANLLWYTH, 3 PERIODS IN 1986, COMPARISON OF EP WITH MEASURED DAILY NET RAINFALL

There is a need to test the simulated EP values against measured net rainfall. However, suitable measured net rainfall data sets are scarce. Measured daily

data were obtained from an experimental site at Plynlimon, where net rainfall has been derived from below-canopy gauges (P.T.W. Rosier, personal communication). Three time periods were simulated, namely (i) 7–12 June, (ii) April and (iii) August, all in 1986. AWS and catchment data for Tanllwyth were used. Catchment parameters specified were PLAI = 0.92 and HVEG = 10.0 m (observed estimates), CLAI = 2.0 and CMAX = 2.0 mm.

The good agreement between modelled and measured net rainfall for the June data (Figure 5) gave confidence that a reasonable fit would also be simulated for the April and August data. This was subsequently found to be the case, illustrating the predictive qualities of the model (Figures 6 and 7). Good agreement between the peaks was obtained. The model generated  $\Sigma EP = 38\%$  of  $\Sigma RF$  for June (compared with a measured total net rainfall of  $\Sigma_{net} = 53\%$  of  $\Sigma RF$ ),  $\Sigma EP = 50\%$  of  $\Sigma RF$  for April (compared with 60%), and  $\Sigma EP = 45\%$  of  $\Sigma RF$  for August (compared with 59%). These values can be compared with modelled values of 82–86% for the storms of 7–8/2/76 and 1/11/77 for Tanllwyth, and with 70% for 5-year means for the Severn catchment (Table 1). This comparison suggests that there may exist both a seasonal effect (in that EP as a percentage of RF is reduced in summer) and an averaging effect (in that EP as a percentage of RF may be reduced in a longer-term study compared with a short period of storm rainfall), which intuitively seem to be correct.

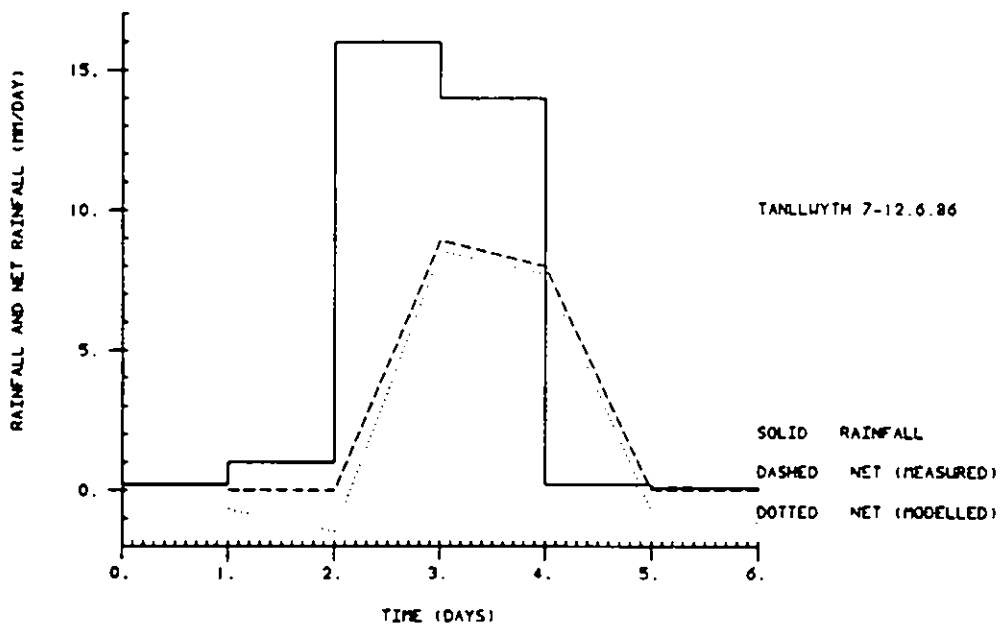


**Figure 5** Rainfall and modelled net rainfall (for grass and forest) against time for the storm of 7-12/6/86 on the Tanllwyth catchment.

For the measured data, stemflow has been estimated to account for 30% of average net rainfall. However, stemflow is not explicitly incorporated in the present model and hence values of EP are expected to give an underestimate

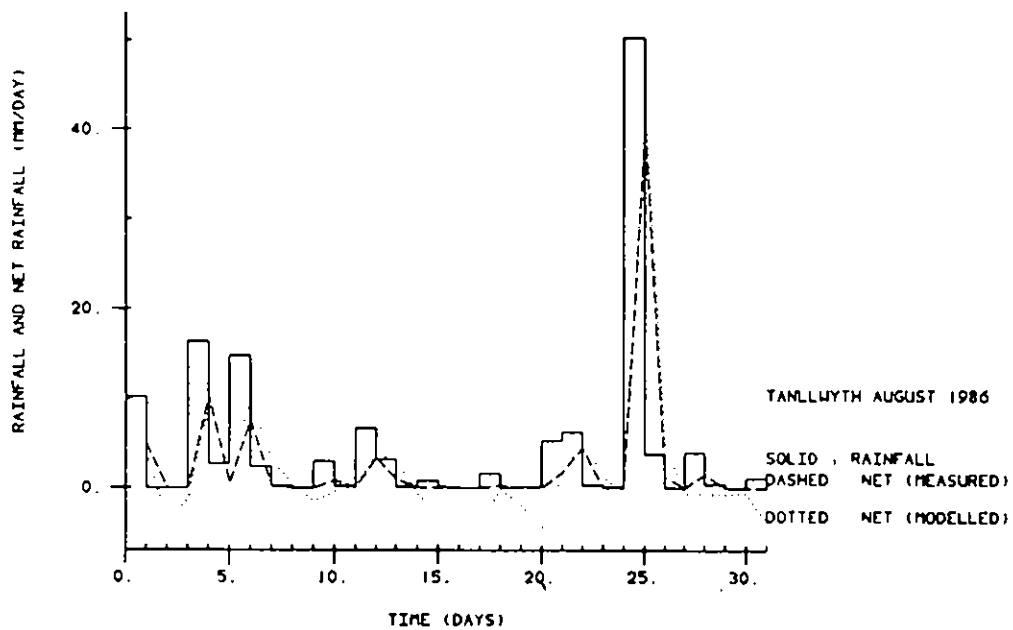


Figure 6 Rainfall, measured and modelled net rainfall against time for the Tanllwyth catchment, August 1986.

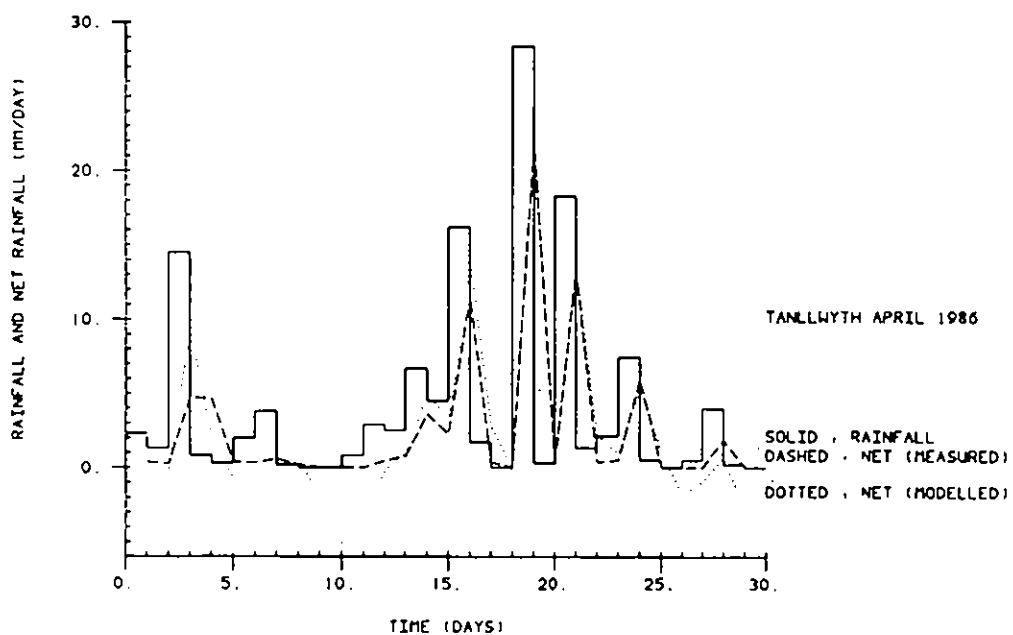


Figure 7 Rainfall, measured and modelled net rainfall against time for the Tanllwyth catchment, April 1986.

of the net rainfall. Although a reasonable agreement of EP with net rainfall has been derived,  $\Sigma EP$  is still only 80% of  $\Sigma_{net}$  (though compared with an expected  $\Sigma EP$  of only 70% of  $\Sigma_{net}$ ). The additional 10% simulated is because drip-drain from the canopy is being modelled rather than stemflow, and this may suggest that in this study roughly one-third of stemflow is incorporated in the simulations. Further, simulated EP has some negative values, representing potential evapotranspiration, which the net rainfall data do not account for. If potential evapotranspiration cannot be sustained, then the potential negative values will not be met.

Negative values for EP are acceptable since high potential evapotranspiration rates may be expected when surface temperatures are high and input RF low. Thom and Oliver (1977) suggest possible evaporation rates of 5 mm day<sup>-1</sup> from a wet canopy in winter. Allowing for an interception rate of 2-3 mm day<sup>-1</sup>, this indicates an evapotranspiration rate of 2-3 mm day<sup>-1</sup>. Gash *et al.* (1980) present a typical evaporation rate of 0.22 mm hr<sup>-1</sup> (5.28 mm day<sup>-1</sup>) as an average for British forests. If all EP predictions are assumed to equal or exceed zero, then  $\Sigma EP = 68\%$  of  $\Sigma RF$  is derived for both April and August simulations. This indicates that somewhat more than 50% of potential moisture requirements would be provided by the upper root zone of the unsaturated zone of this study. From inspection of the EP data, this corresponds to 2 mm day<sup>-1</sup> of moisture. Assuming that the unsaturated zone may indeed provide up to 2 mm day<sup>-1</sup> of moisture, the model was able to simulate agreement of EP to net rainfall to within  $\pm 2\%$ , thus indicating a possible method for linking the preprograms to the main IHDM.

Some additional explanations for the discrepancy between EP and net rainfall may also be suggested. First, parameters such as HVEG may benefit from further adjustment. Second, RF has been assumed constant throughout each day, since only daily values were available, but this may be inadequate. Third, zero interception store has been assumed at the start of the simulation. Fourth, variables such as temperature may not be the same at the study site as at the AWS. Fifth, the model may still be too simplified to derive improved agreement between EP and net rainfall.

### 3.9 TANLLWYTH, 11-12/1/80, USING RAIN AND SNOW MODEL

This simulation was performed to demonstrate the potential of using the interception-evapotranspiration model in conjunction with the snow model. For snowfall to be simulated, the model requires data in which RF occurs, temperatures fall below zero, and an initial snow cover, WE0, exists. This study used a negligible initial thickness of this snow cover, WE0 = 10<sup>-6</sup>m, and hourly AWS data. Other parameters were specified as in section 3.8.

$\Sigma RF$  was 10.0 mm and the total EP for the rain only model ( $\Sigma EP_R$ ) was 5.5 mm compared to the total EP for the combined rain and snow model ( $\Sigma EP_{R+S}$ ) of 3.6 mm. These values seem reasonable since most RF falls as snow because temperatures are generally below zero and a thin snow layer builds up. Figure 8 shows that until t=14 hours some evapotranspiration is simulated in the rain model. For the first five peaks in RF it is evident

that most RF is intercepted but that the interception store is steadily filled since values of EP are increasing. Following each peak, some delayed runoff is simulated. The highest peak in RF occurs at  $t=36$  h, corresponding to mid-day on 12 January. At  $t=36$  h,  $EP_{R+S}$  exceeds both RF and  $EP_R$ , because rainfall is supplemented by melting of the existing snow layer. The peak in  $EP_{R+S}$  occurs soon after the peak in RF, whereas the peak in  $EP_R$  is delayed longer. Following the main peaks, RF exceeds  $EP_{R+S}$  indicating that the snowpack depth is increasing. There is a longer tail in  $EP_R$  compared with  $EP_{R+S}$ .

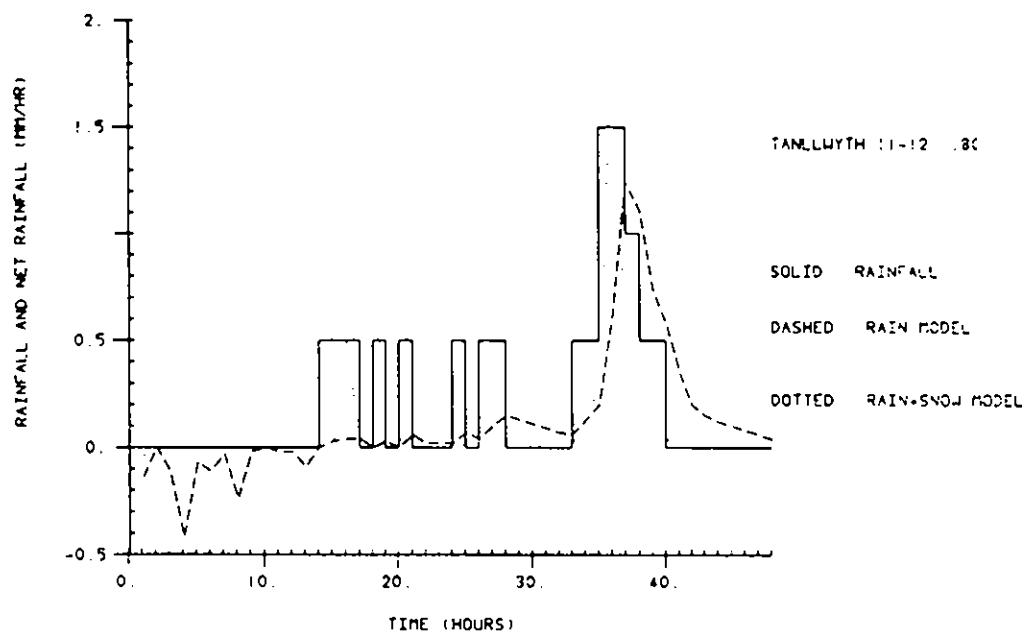


**Figure 8** Rainfall and modelled net precipitation (for rain only model and rain + snow model) against time for the storm of 11-12/1/80 on the Tanllwyth catchment.

## 4. Comment

The IHDM uses rainfall as model input to generate predicted stream hydrographs as output. This report provides information on the development and application of the IHDM preprograms, which are designed to provide improved estimates of net rainfall for input to the IHDM. However, as noted in section 1, the preprograms are not restricted to use solely in conjunction with the IHDM.

Although research is continuing, the case study simulations already indicate that the IHDM preprograms form important components of the IHDM. These case studies have demonstrated the potential of the preprograms for (i) grassland studies, (ii) forest studies, (iii) extended time period studies, (iv)



studies of complex catchments requiring simulation with many different zones, (v) the use of areal catchment rainfall or stream gauge rainfall in conjunction with AWS data, (vi) the use of daily AWS data when hourly data is unavailable, (vii) a comparative study of simulated net rainfall with measured net rainfall, and (viii) the use of a combined rain and snow model. The good agreement obtained between measured and modelled net rainfall generates confidence in the predictive qualities of the modelling. The organisation of the preprograms allows for many potential improvements which may be implemented according to the specific requirements of the particular user.

## 5 Acknowledgements

The IHDM project is funded by the Ministry of Agriculture, Fisheries and Food. Model development and data provision are the result of the efforts of many Institute of Hydrology personnel, whose contributions are gratefully acknowledged. In particular, the guidance of A. Calver has been valuable. The modelling studies of K. J. Beven and E. M. Morris have provided the foundation to this report.

## 6. References

- Anon. 1976. Water balance of the headwater catchments of the Wye and Severn, 1970-1975. *Institute of Hydrology Report No. 33*.
- Beven, K. 1979. A sensitivity analysis of the Penman-Monteith actual evapotranspiration estimates. *Journal of Hydrology*, **44**, 169-190.
- Beven, K. J., Calver, A. and Morris E. M. 1987. The Institute of Hydrology Distributed Model. *Institute of Hydrology Report No. 98*.
- Brunt, D. 1932. Notes on radiation in the atmosphere. *Quarterly Journal of the Royal Meteorological Society*, **58**, 389-420.
- Calder, I. R. 1977. A model of transpiration and interception loss from a spruce forest in Plynlimon, central Wales. *Journal of Hydrology*, **33**, 247-265.
- Calver, A. 1988. Calibration, sensitivity and validation of a physically-based rainfall-runoff model. *Journal of Hydrology*. (In press).
- Gash, J. H. C., Wright, I. R. and Lloyd. C. R. 1980. Comparative estimates of interception loss from three coniferous forests in Great Britain. *Journal of Hydrology*, **48**, 89-105.

- Monteith, J. L. 1965. Evaporation and environment. *Symposia Society Experimental Botany*, 19, 205-234.
- Morris, E. M. 1983. Modelling the flow of mass and energy within a snowpack for hydrological forecasting. *Annals of Glaciology*, 4, 198-203.
- Morris, E. M. 1985. Snow and ice. In: Anderson, M. G. and Burt, T. P. (eds.), *Hydrological Forecasting*, Wiley, London 153-182.
- Rutter, A. J., Kershaw, K. A., Robins, P. C. and Morton, A. J. 1971. A predictive model of rainfall interception in forests I: Derivation of the model from observations in a plantation of Corsican pine. *Agricultural Meteorology*, 9, 367-384.
- Rutter, A. J. and Morton, A. J. 1977. A predictive model of rainfall interception in forests III: Sensitivity of the model to stand parameters and meteorological variables. *Journal of Applied Ecology*, 14, 567-588.
- Sellers, W. D. (1965). *Physical Climatology*. Chicago Press, Chicago. USA, 272pp.
- Thom, A. S. and Oliver, H. R. 1977. On Penman's equation for estimating regional evaporation. *Quarterly Journal of the Royal Meteorological Society*, 103, 345-357.



